

**Adsorption and diffusion of water on graphene from first principles**Jie Ma,<sup>1</sup> Angelos Michaelides,<sup>2,\*</sup> Dario Alfè,<sup>3</sup> Laurids Schimka,<sup>4</sup> Georg Kresse,<sup>4</sup> and Enge Wang<sup>5,1</sup><sup>1</sup>*Institute of Physics, Chinese Academy of Sciences, Box 603, Beijing 100190, China*<sup>2</sup>*London Centre for Nanotechnology & Department of Chemistry, University College London, London WC1H 0AJ, UK*<sup>3</sup>*Department of Earth Sciences & Department of Physics and Astronomy & London Centre for Nanotechnology, London, UK*<sup>4</sup>*University of Vienna, Faculty of Physics and Center for Computational Materials Science, Vienna, Austria*<sup>5</sup>*School of Physics, Peking University, Beijing 100871, China*

(Received 6 May 2011; published 1 July 2011)

Water monomer adsorption on graphene is examined with state-of-the-art electronic structure approaches. The adsorption energy determinations on this system from quantum Monte Carlo and the random-phase approximation yield small values of  $<100$  meV. These benchmarks provide a deeper understanding of the reactivity of graphene that may underpin the development of improved more approximate methods enabling the accurate treatment of more complex processes at wet-carbon interfaces. As an example, we show how dispersion-corrected density functional theory, which we show gives a satisfactory description of this adsorption system, predicts that water undergoes ultra-fast diffusion on graphene at low temperatures.

DOI: [10.1103/PhysRevB.84.033402](https://doi.org/10.1103/PhysRevB.84.033402)

PACS number(s): 68.43.Bc, 31.15.em, 68.43.Fg, 82.65.+r

There is great interest in exploring the interaction of water with carbon, such as graphene, graphite, or carbon nanotubes. This comes from a desire to understand phenomena such as lubrication, heterogeneous ice nucleation, the properties and function of carbon nanotubes in biological media, the structural and phase behavior of water at the nanoscale, to name but a few.<sup>1,2</sup> However, at the molecular level, understanding is far from complete with the most fundamental matter of how strong the bond is between water molecules and any carbon surface yet to be established. This seemingly simple issue is at the foundation of our understanding of water-carbon interfaces, illustrated, for example, by simulations of water in carbon nanotubes. Empirical potential calculations with one choice of water-carbon interaction predict filled tubes, but with another, involving a minute reduction in the attraction between water and the tube wall, almost empty tubes.<sup>3</sup> Likewise, other simulations show that a small variation in the strength of the water-carbon bond leads graphite surfaces to appear as hydrophobic, but with another hydrophilic.<sup>4</sup> Clearly, if progress is to be made in interpreting experiments or in accurately simulating complex wet-carbon interfaces, a reliable value for the bond strength between water and carbon is essential.

Establishing reliable adsorption energies for water monomers is a major challenge for both experiment and theory. Experiment is stymied because water forms clusters. Theory finds it difficult because water interacts with materials via dispersion [van der Waals (vdW)] and hydrogen bonding. These are interactions which density functional theory (DFT), the most widely used electronic structure theory, does not normally describe with enough precision. With this in mind, water on graphite or graphene has been used as a model system with which to benchmark the water-carbon bond strength.<sup>5–12</sup> Traditionally, fused benzene rings (a finite cluster model) have been adopted, enabling the application of explicitly correlated quantum chemistry approaches. Adsorption energies from these approaches range from  $-100$  meV to more than  $-200$  meV,<sup>5,7,9</sup> with recent values being about  $-130$  to  $-140$  meV.<sup>11,12</sup> However, these calculations do not involve truly extended models for graphene and hence *a priori* neglect correlation contributions from the bands close to the Dirac point.

Recently, diffusion Monte Carlo (DMC) and the random-phase approximation (RPA) to the correlation energy have emerged as exciting alternative approaches that can achieve high accuracy for condensed phase systems (e.g. Refs. 13–15). Indeed, because they can be applied to periodic systems, they have the potential to transform the quality of predictions of adsorption energies. However, so far their application to adsorption has been limited<sup>16</sup> in no small part to their large (RPA) and enormous (DMC) computational cost. Here we present periodic first-principles results for the prototype water-graphene system, using both DMC and RPA. Small values of the adsorption energy of  $<100$  meV are obtained, suggesting that graphene may be less reactive towards water than previously thought. Not only do the benchmark adsorption energies obtained here provide new physical insight, but they also allow us to evaluate the performance of the much cheaper and much more widely used DFT-based approaches. We find that the results from DFT depend strongly on the exchange-correlation functional used, and only when dispersion forces are accounted for does DFT yield reasonable adsorption energies. Using one such dispersion-corrected DFT approach, validated against the accurate reference data, we go on to show that water undergoes ultra-fast diffusion on graphene at low temperatures.

The calculations were performed with several electronic structure codes. Typically graphene is represented by a hexagonal  $5 \times 5$  supercell sampling the electronic structure at the  $\Gamma$  point only. This is large enough to model adsorption of an isolated water monomer. Tests in other cells are also reported. The vacuum spacing between slabs was  $>14$  Å. The DFT calculations used the Car-Parrinello Molecular Dynamics (CPMD) plane-wave code,<sup>17</sup> Troullier–Martins pseudopotentials,<sup>18</sup> and a 100 Ry cutoff. The DMC calculations have been performed with the CASINO code,<sup>13</sup> using structures obtained from DFT with the Perdew-Burke-Ernzerhof exchange-correlation functional.<sup>19</sup> With the longest simulations, the statistical error (one standard deviation) is  $\sim 10$  meV. Further details of the DMC setup are given in Ref. 20; a benchmark study on the water-benzene binding energy curve which showed that the current DMC setup agrees with coupled cluster with

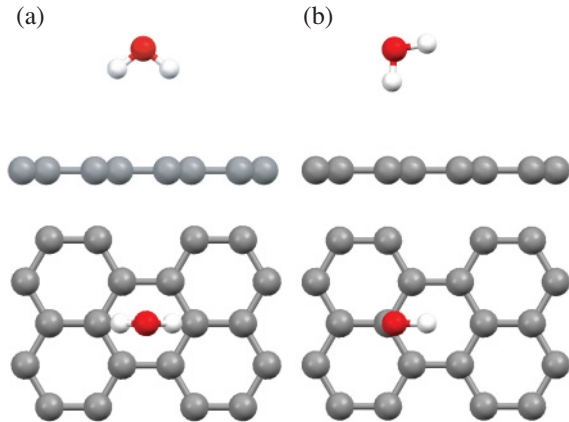


FIG. 1. (Color online) Water adsorption structures considered. (a) The two-leg structure shown from the side (top) and from above (bottom). (b) The one-leg structure shown from the side (top) and from above (bottom). For clarity only a small part of the periodic simulation cell is shown.

single and double excitations plus a perturbative correction for connected triples [CCSD(T)] extrapolated to the complete basis set limit to within 3 meV. The RPA calculations have been performed using the Vienna Ab-initio Simulation Package code, projector-augmented wave potentials and an energy cutoff of 30 Ry. The technical parameters are otherwise similar to recent work on graphite.<sup>15</sup> As a test of RPA on this type of system, calculations were performed for water-benzene finding agreement with Ref. 19 to within 10 meV.

Figure 2 summarizes the binding energy curves for water on graphene obtained with DMC, RPA, and various  $xc$  functionals. Results from two adsorption structures previously discussed in the literature<sup>5,7-9,11,12</sup> are reported. In one structure, referred to as one leg, one of the OH bonds is directed at the surface [Fig. 1(b)]. In the other structure, referred to as two leg, the water is located over the center of a hexagon ring with the two hydrogens equidistant from carbon atoms. The details of the adsorption structure and the adsorption energy  $E_{ads}$ <sup>20</sup> at the minimum of each adsorption energy curve (when there is one) for the various  $xc$  functionals are also given in Table I.

We first discuss the DMC results. About 10 adsorption structures over a range of oxygen heights from 3.0 to 7.2 Å have been computed. Due to the enormous computational cost of DMC, it is not feasible to obtain binding curves with small enough statistical error bars on each data point that allow the precise equilibrium height and exact  $E_{ads}$  to be determined. Nonetheless, it is clear that  $E_{ads}$  for the two-leg structure is about  $-70$  meV and for the one-leg structure around  $-60$  meV, with the equilibrium height in each case  $\sim 4.0$  Å. For both structures, there is a small dip in the binding energy at 6.0–6.5 Å. The origin of this putative minimum is unclear; it may be due to statistical errors or to the presence of a second shallow minimum at large water-graphene distance.

The RPA calculations were initially performed in the  $5 \times 5$  unit cell, yielding  $E_{ads}$  of  $-81$  and  $-77$  meV for the one-leg and two-leg structures, respectively, in good agreement with DMC. The main difference from DMC is a slight shift towards smaller water-graphene distances and the absence of the shallow minimum at large distances. To converge the

TABLE I. Adsorption energy  $E_{ads}$  and height (O-graphene perpendicular distance) for the one- and two-leg configurations of water on graphene (see Fig. 1) with various methods. For DMC an error bar of  $\sim 10$  meV is also given based on the range of values obtained at the broad minimum of the DMC binding energy curve. RPA values in parenthesis are for the  $5 \times 5$  unit cell, the others are obtained with a combination of  $2 \times 2$  and  $8 \times 8$  unit cells for the correlation and Hartree-Fock energies, respectively, as described in the text. BLYP and B3LYP yield purely repulsive binding energy curves (Fig. 2) and so are not reported here.

Approach	Two leg		One leg	
	$E_{ads}$ (meV)	Height (Å)	$E_{ads}$ (meV)	Height (Å)
DMC	$-70 \pm 10$	3.4-4.0	$-70 \pm 10$	3.4-4.0
RPA	$-98$ ( $-77$ )	3.42	$-82$ ( $-81$ )	3.55
LDA	$-151$	3.04	$-139$	3.15
PBE	$-27$	3.65	$-31$	3.65
PBE0	$-23$	3.62	$-27$	3.66
revPBE	$-4$	4.66	$-7$	4.42
PBE-D	$-90$	3.35	$-87$	3.45
BLYP-D	$-90$	3.35	$-87$	3.47

results with respect to Brillouin zone sampling, we performed additional calculations for a  $4 \times 4$  cell using  $2 \times 2 \times 1$   $k$  points and a  $2 \times 2$  cell with up to  $8 \times 8 \times 1$   $k$  points. The changes of the correlation energy upon adsorption of water are identical to within 5 meV for the  $4 \times 4$  and  $2 \times 2$  cell, if identical  $k$ -point spacings are used. This indicates that correlation energy differences are fairly independent of coverage. Although the same is not observed for other contributions to the total energy (kinetic, Hartree, and exact-exchange energy), we can obtain very accurate results by combining the correlation energies for a  $2 \times 2$  cell using  $8 \times 8 \times 1$   $k$  points with the Hartree-Fock energy evaluated for a larger  $8 \times 8$  cell and  $2 \times 2 \times 1$   $k$  points (Table I). Further test calculations indicate that these results are converged to better than 10 meV. The differences to the straightforward  $5 \times 5$  calculations (applying the  $\Gamma$  point only) depend on the orientation of the  $H_2O$  molecule. For the two-leg structure, the  $5 \times 5$  calculation underestimates the binding energy by 20 meV, whereas for the one-leg structure the results for the  $5 \times 5$  unit cell are practically identical to the more accurate results. Since  $k$ -point convergence is expected to be similar for RPA and DMC, we expect that the converged DMC binding energy for the two-leg structure is about  $-90$  meV.

The RPA correlation energy is sufficiently smooth to analyze its analytical behavior. As expected for the interaction between an insulating (or semiconducting) sheet and a molecule, the correlation energy is, to a good approximation, proportional to  $15 \text{ eV} \text{ \AA}^4 / (d - 0.25 \text{ \AA})^4$ , where  $d$  is the distance between the O atom and the graphene slab; the center of polarizability of the water molecules is obviously shifted towards the H atoms. Due to the large supercell and the limited vacuum width, analysis at very large distances, as done for graphite,<sup>15</sup> is presently not possible. However, at the intermediate distances considered here, a simple pairwise additive  $R^{-6}$  potential between individual carbon atoms and the water molecule is compatible with the calculated  $1/d^4$  behavior. This suggests that the use of a pairwise additive  $C_6 R^{-6}$  (where  $R$  is distance between two atoms) correction

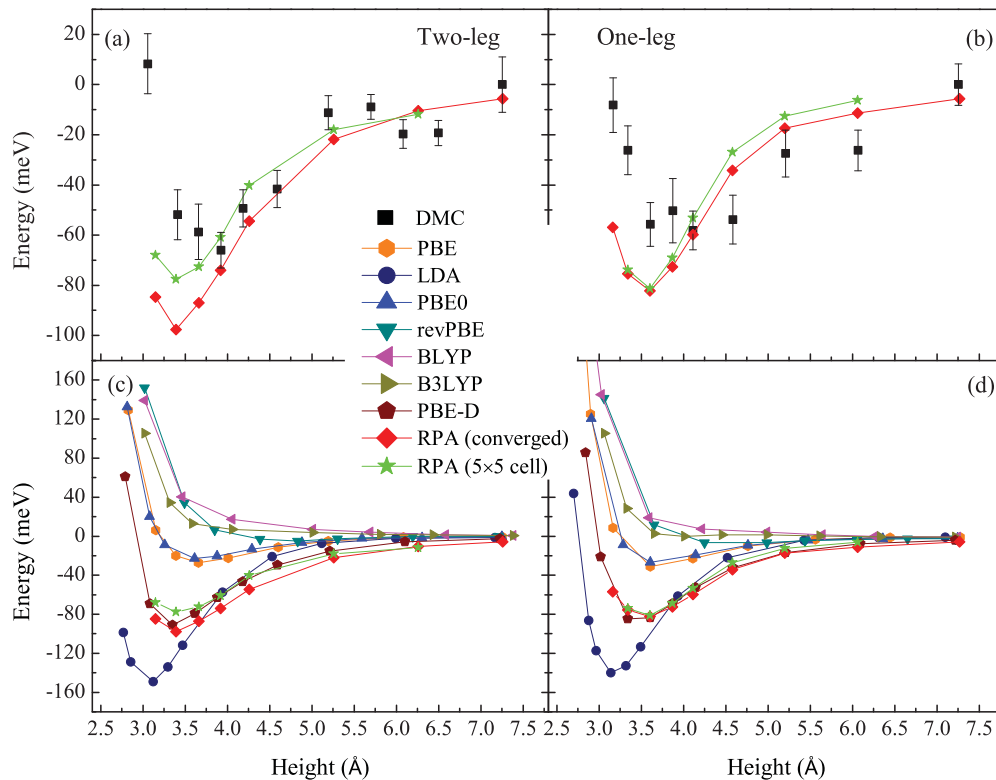


FIG. 2. (Color online) Adsorption energy versus O atom height for water on graphene obtained with various methods. (a) and (c) The two-leg configuration. (b) and (d) The one-leg configuration. In the upper panels, DMC and RPA are compared. In the lower panels, RPA and the various  $xc$  functionals are compared.

should yield accurate results. The RPA calculations and the simple analytic behavior up to 7 Å from the surface also suggest that the shallow DMC minimum at large distances is likely a sampling artifact rather than a real physical feature.

Having established reference values of  $-70$  to  $-98$  meV from DMC and RPA, it is interesting to briefly assess the performance of certain DFT  $xc$  functionals, not least because DFT is currently the method of choice in first-principles studies of water adsorption. First and foremost, it is clear from Figs. 2(c) and 2(d) that the different  $xc$  functionals give very different results with the predicted  $E_{ads}$  ranging from zero to about  $-150$  meV. Not surprisingly, for both configurations, LDA gives the largest  $E_{ads}$  and smallest adsorption height ( $\sim 3$  Å). PBE is a very popular  $xc$  functional,<sup>21</sup> widely used in water adsorption studies. Here PBE gives an  $E_{ads}$  of  $-31$  meV, with the difference in  $E_{ads}$  between the two configurations being only 4 meV. The shallow adsorption minima are at around 3.65 Å for both configurations, about 0.6 Å higher than the LDA value. One of the revised versions of PBE, revPBE,<sup>22</sup> predicts nearly no binding, and the hybrid version of PBE, PBE0,<sup>23</sup> predicts curves that are almost indistinguishable from PBE. Becke–Lee–Yang–Parr (BLYP) is widely used for liquid water.<sup>24,25</sup> However, in this system, BLYP predicts a repulsive interaction for both configurations. Likewise, Becke 3-parameter Lee–Yang–Parr (B3LYP),<sup>24–28</sup> the hybrid functional, predicts no binding whatsoever to the surface.

The DFT results strongly depend on the  $xc$  functional used with none of the functionals coming even within 20–30% of

the reference energies. Furthermore, all functionals considered decay exponentially at large distances and fail to predict the correct  $1/d^4$  medium-range behavior. This poor performance is due to the inadequacies of standard  $xc$  functionals in treating vdW forces. Strategies for dealing with vdW forces within DFT are usually based on  $xc$  functionals that explicitly account for nonlocal correlation or empirical  $C_6R^{-6}$  corrections dispersion (DFT-D).<sup>29–32</sup> Considering the RPA binding curve with an almost perfect  $1/d^4$  behavior, DFT-D seems to be a good choice for correcting for the deficiencies of DFT. This has been done for both the PBE and the BLYP functionals by adopting Grimme’s protocol.<sup>31</sup> The calculated adsorption energies and structures obtained from DFT-D with the PBE and BLYP functionals are shown in Table I. Since both curves are similar, we only plot the PBE-D curve in Figs. 2(c) and 2(d). The first general conclusion is that this vdW correction scheme outperforms the regular  $xc$  functionals with reasonably good agreement with DMC and RPA. The agreement with the RPA and the  $k$ -point corrected DMC results is in fact excellent, and even the slight preference for the two-leg structure is reproduced. In particular, the equilibrium distances as well as the long-range behavior are in very reasonable agreement with RPA. This suggests that DFT-D is capable of recovering the essential physics of this adsorption system with a computational effort that is several orders of magnitude less than that of RPA and DMC.

The improved performance of DFT-D over the standard  $xc$  functionals allows the dynamical properties of the water monomer on graphene to be briefly considered. To this end, we

have performed molecular dynamics (MD) simulations with the PBE-D approach at 100 K (a low enough temperature to inhibit water desorption).<sup>33</sup> During the simulation, the water molecule undergoes a random walk, and the estimated diffusion coefficient is 0.6 Å<sup>2</sup>/ps. This is about an order of magnitude greater than the self-diffusion coefficient of liquid water and indicates an ultra-fast diffusion of the water monomer. This result relates well to the observation made in the introduction: it will be difficult to determine the adsorption energy of isolated water molecules experimentally, since diffusion on graphene is so rapid that water molecules will always agglomerate and form larger hydrogen-bonded clusters.

In conclusion, we have obtained the first explicitly correlated results (from both DMC and RPA) for adsorption on a periodic graphene sheet. From DMC and RPA a value of −70 to −98 meV has been obtained for each of the two water configurations tested with a slight preference for a structure with two hydrogens oriented towards the surface. These values are below the range obtained from calculations on cluster models. The rather close agreement between DMC and RPA suggests that our values can serve as valuable benchmarks and aid in the development of improved approximate methods for treating the water-carbon interface, such as new DFT *xc* functionals and force fields. Aside from providing a long

sought-after benchmark on a periodic graphene sheet, we have examined how some of the most popular DFT *xc* functionals used in water adsorption studies perform for this system. None of the functionals considered provide a satisfactory description of the water-graphene interaction, unless dispersion forces are accounted for. Using the empirical DFT-D scheme we find, through MD simulations, that water monomers undergo ultra-fast diffusion on graphene at low temperatures. Such dispersion-corrected DFT schemes provide a relatively cheap and pragmatic scheme for obtaining improved accuracy for complex systems beyond the reach of DMC and RPA, such as liquid water graphene interfaces or carbon nanotubes immersed in water.

JM and EGW are supported by NSFC, and AM and DA by the EURYI scheme and EPSRC. AM is also supported by ERC. LS and GK acknowledge funding by the Austrian science fund (FWF) through the WK CMS (W401) and the SBF ViCoM (F41). We are grateful for computer time through the DEISA initiative and time on JaguarPF through the US Department of Energy INCITE program, as well as compute time on the Vienna Scientific Cluster (VSC). JM is grateful to the Thomas Young Centre for a Junior Research Fellowship. Valuable discussions with John Dobson and Angel Rubio are also warmly acknowledged.

\*angelos.michaelides@ucl.ac.uk

<sup>1</sup>K. Falk, F. Sedlmeier, L. Jolly, R. R. Netz, and L. Bocquet, *Nano Lett.* **10**, 4067 (2010).

<sup>2</sup>L. Bocquet and E. Charlaix, *Chem. Soc. Rev.* **39**, 1073 (2010).

<sup>3</sup>G. Hummer, J. C. Rasaiah, and J. P. Noworyta, *Nature* **414**, 188 (2001).

<sup>4</sup>T. Werder, J. H. Walther, R. L. Jaffe, T. Halicioglu, and P. Koumoutsakos, *J. Phys. Chem. B* **107**, 1345 (2003).

<sup>5</sup>D. Feller and K. D. Jordan, *J. Phys. Chem. A* **104**, 9971 (2000).

<sup>6</sup>H. Ruuska and T. A. Pakkanen, *Carbon* **41**, 699 (2003).

<sup>7</sup>I. W. Sudiarta and D. J. W. Geldart, *J. Phys. Chem. A* **110**, 10501 (2006).

<sup>8</sup>C. S. Lin, R. Q. Zhang, S. T. Lee, M. Elstner, T. Frauenheim, and L. J. Wan, *J. Phys. Chem. B* **109**, 14183 (2005).

<sup>9</sup>S. Xu, S. Irle, D. G. Musaev, and M. C. Lin, *J. Phys. Chem. A* **109**, 9563 (2005).

<sup>10</sup>G. R. Jenness and K. D. Jordan, *J. Phys. Chem. C* **113**, 10242 (2009).

<sup>11</sup>M. Rubeš, P. Nachtigall, J. Vondrasek, and O. Bludsky, *J. Phys. Chem. C* **113**, 8412 (2009).

<sup>12</sup>G. R. Jenness, O. Karalti, and K. D. Jordan, *Phys. Chem. Chem. Phys.* **12**, 6375 (2010).

<sup>13</sup>R. J. Needs, M. D. Towler, N. D. Drummond, and P. Lopez Rios, *J. Phys.: Condens. Matter* **22**, 023201 (2010).

<sup>14</sup>J. Harl and G. Kresse, *Phys. Rev. Lett.* **103**, 056401 (2009).

<sup>15</sup>S. Lebègue, J. Harl, T. Gould, J. G. Angyan, G. Kresse, and J. F. Dobson, *Phys. Rev. Lett.* **105**, 196401 (2010).

<sup>16</sup>L. Schimka, J. Harl, A. Stroppa, A. Grüneis, M. Marsman, F. Mittendorfer, and G. Kresse, *Nature Mater.* **9**, 741 (2010).

<sup>17</sup>CPMD, [<http://www.cpmd.org/>], Copyright IBM Corp 1990–2008, Copyright MPI für Festkörperforschung Stuttgart 1997–2001.

<sup>18</sup>N. Troullier and J. L. Martins, *Phys. Rev. B* **43**, 1993 (1991).

<sup>19</sup>J. Ma, D. Alfè, A. Michaelides, and E. G. Wang, *J. Chem. Phys.* **130**, 154303 (2009).

<sup>20</sup>For DFT and RPA the adsorption energy is defined as  $E_{ads} = E_{water/graphene} - E_{water} - E_{graphene}$ , where  $E_{water/graphene}$ ,  $E_{graphene}$ , and  $E_{water}$  are the total energies of the water-graphene system, clean graphene, and the isolated water, respectively. In DMC  $E_{ads} = E_{water/graphene} - E_{water-far/graphene}$ , where  $E_{water-far/graphene}$  is the total energy of the water/graphene system with the largest water-graphene separation considered ( $\sim 7$  Å).

<sup>21</sup>J. P. Perdew, K. Burke, and M. Ernzerhof, *Phys. Rev. Lett.* **77**, 3865 (1996).

<sup>22</sup>Y. Zhang and W. Yang, *Phys. Rev. Lett.* **80**, 890 (1998).

<sup>23</sup>C. Adamo and V. Barone, *J. Chem. Phys.* **110**, 6158 (1999).

<sup>24</sup>A. D. Becke, *Phys. Rev. A* **38**, 3098 (1988).

<sup>25</sup>C. Lee, W. Yang, and R. G. Parr, *Phys. Rev. B* **37**, 785 (1988).

<sup>26</sup>A. D. Becke, *J. Chem. Phys.* **98**, 5648 (1993).

<sup>27</sup>S. H. Vosko, L. Wilk, and M. Nusair, *Can. J. Phys.* **58**, 1200 (1980).

<sup>28</sup>P. J. Stephens, F. J. Devlin, C. F. Chabalowski, and M. J. Frisch, *J. Phys. Chem.* **98**, 11623 (1994).

<sup>29</sup>M. Dion, H. Rydberg, E. Schroder, D. C. Langreth, and B. I. Lundqvist, *Phys. Rev. Lett.* **92**, 246401 (2004).

<sup>30</sup>J. Klimeš, D. R. Bowler, and A. Michaelides, *J. Phys.: Condens. Matter* **22**, 022201 (2010).

<sup>31</sup>S. Grimme, *J. Comput. Chem.* **25**, 1463 (2004).

<sup>32</sup>J. Klimeš, D. R. Bowler, and A. Michaelides, *Phys. Rev. B* **83**, 195131 (2011).

<sup>33</sup>In the  $\sim 10$  ps canonical ensemble MD simulations deuterium masses were used, a 1 fs timestep, and a Nosé–Hoover chain thermostat.